

UC San Diego

UC San Diego Previously Published Works

Title

1,4-Dihydropyridinebutyrolactone-derived ring-opened ester and amide analogs targeting BET bromodomains.

Permalink

<https://escholarship.org/uc/item/2pj2b7ff>

Journal

Archiv der Pharmazie, 355(11)

Authors

Jiang, Jiewei

Zhao, Pei-Liang

Sigua, Logan

et al.

Publication Date

2022-11-01

DOI

10.1002/ardp.202200288

Peer reviewed



Published in final edited form as:

Arch Pharm (Weinheim). 2022 November ; 355(11): e2200288. doi:10.1002/ardp.202200288.

1,4-Dihydropyridinebutyrolactone-derived ring-opened ester and amide analogs targeting BET bromodomains

Jiewei Jiang^{a,#}, Pei-Liang Zhao^{a,#}, Logan H. Sigua^b, Alice Chan^c, Ernst Schönbrunn^c, Jun Qi^{b,d}, Gunda I. Georg^a

^aDepartment of Medicinal Chemistry and Institute for Therapeutics Discovery and Development, College of Pharmacy, University of Minnesota, Minneapolis, MN, USA

^bDepartment of Cancer Biology, Dana-Farber Cancer Institute, Boston, MA, USA

^cMoffitt Cancer Center, Drug Discovery Department, Tampa, FL, USA

^dDepartment of Medicine, Harvard Medical School, Boston, MA, USA

Abstract

Based on a previously reported 1,4-dihydropyridinebutyrolactone virtual screening hit, nine lactone ring-opened ester and seven amide analogs were prepared. The analogs were designed to provide interactions with residues at the entrance of the ZA channel to enhance the affinity and selectivity for BET bromodomains. Compound testing by AlphaScreen showed that neither the affinity nor the selectivity of the ester and lactam analogs was improved for BRD4-1 and BRDT-1. The esters retained affinity comparable to the parent compound, whereas the affinity for the amide analogs was reduced 10-fold. A representative benzyl ester analog was found to retain high selectivity for BET bromodomains as shown by a BROMOScan. X-ray analysis of the allyl ester analog in complex with BRD4-1 and BRDT-1 revealed that the ester side chain is located next to the ZA loop and solvent exposed.

Keywords

AlphaScreen; bromodomain and extra-terminal (BET) proteins; BET selectivity; BROMOScan; X-ray

1 INTRODUCTION

Bromodomain-containing proteins are a family of “reader” proteins that specifically recognize the acetylated lysine (Kac) residues in histone tails during post-translational processes.^[1] To date, 46 proteins have been identified to have 61 bromodomains that are classified into 8 subfamilies.^[2] The bromodomain and extra-terminal (BET) have been most extensively investigated. The BET subfamily comprises BRD2, BRD3, and BRD4 as well

*Correspondence: Gunda I. Georg, Department of Medicinal Chemistry and Institute for Therapeutics Discovery and Development, College of Pharmacy, University of Minnesota, 717 Delaware Street, SE, Minneapolis, MN 55414, USA, georg@umn.edu.

#These authors contributed equally

CONFLICT OF INTEREST

The authors have declared no conflict of interest.

as testis restricted BRDT.^[2, 3] The BET proteins have two tandem bromodomains (BD1 and BD2), both of which recognize Kac moieties with varying affinities, depending on the locations as well as acetylation levels of lysine residues.^[2] The four BET proteins also have an extra-terminal (ET) domain near the C-terminus, responsible for interaction with chromatin and transcription proteins.^[4–6] The eight bromodomains share moderate to high sequence and protein folding similarity within the BET family. There are four alpha helices (α A, α Z, α B, and α C) that are connected via two flexible loop regions (ZA and BC loops). Surrounded by two loops is a cavity in the middle of four helical bundles, inside of which are several structurally conserved water molecules stabilizing the protein fold via a hydrogen bond network. Upon interaction with acetylated histones, BET proteins recruit various components (i.e., positive transcriptional elongation factor b,^[7] lysine methyltransferase,^[8] and Jumonji domain-containing protein 6^[9]) to assemble the transcriptional machinery and initiate gene expression.^[10] Because of their pivotal role in epigenetic processes, inhibition of BET proteins can be exploited for the discovery of novel therapeutics. For instance, BRD4 inhibition downregulates the expression of c-Myc,^[11] an oncogene frequently amplified or overexpressed in leukemia, myeloma and lymphoma.^[12–14] As such, various BRD4 inhibitors are being explored as potential cancer therapeutics. Meanwhile, BRDT is crucial for spermatogenesis based on knockout studies and mouse mating studies performed with pan-BET inhibitor JQ1 (Figure 1).^[15, 16] As such, selective BRDT inhibitors hold promise as novel male contraceptives.^[3, 15, 17, 18] BET inhibitors (Figure 1) achieve their pharmacological activity by outcompeting the endogenous Kac moieties of acetylated lysine recognition sites.^[19–21] Most small molecule inhibitors occupy the highly conserved Kac recognition pockets with minimal preference within the BET subfamily.^[22] However, several selective inhibitors have been discovered.^[23–27] Examples are BD1 inhibitor GSK778 and BD2 inhibitor GSK046,^[28] BD2 inhibitor ABBV-744^[29] and BRDT-2-selective inhibitor CD1102^[18] Because BET proteins have two tandem bromodomains, simultaneous occupancy of both BD1 and BD2 was achieved with bivalent small molecule inhibitors such as MT1 (Figure 1).^[30, 31] Besides occupancy-driven inhibition, targeted protein degradation of BET proteins via hijacking the proteasome system has also been reported, in which pan-BET inhibitor JQ1 was connected to an E3 ligase recruiting motif via either a PEG or a hydrocarbon linker (ARV-825, Figure 1).^[32, 33] Despite progress in the development of potent BET inhibitors, mixed clinical outcomes such as dose-dependent toxicities (DLTs)^[34–37] and drug resistance^[38–40] are concerns for BET inhibitors for cancer therapy. Although the cause of drug resistance remains elusive, DLTs are believed to arise from pan-BET inhibition.

2 RESULTS AND DISCUSSION

From a virtual screen of over 6 million compounds, we previously identified a tricyclic, dihydropyridine scaffold (**1**, Figure 2B), which displayed promising activity against the BET family.^[41] Preliminary structural modifications on the uracil moiety and the aryl group did not provide analogs with improved affinity. Crystallographic data and computational studies indicated that opening the lactone ring might direct the ester/amide side chain to the entrance of the ZA channel and thus interact with surrounding residues, which might be advantageous for BET affinity (Figure 2A). Furthermore, we previously proposed an

arginine hypothesis, whereby leveraging the unique arginine 54 (R54, Figure 2C) in the ZA channel of BRDT-1, BRDT specificity might be achieved.^[42] Herein, we embarked on the evaluation of lactone ring-open modifications of original hit compound **1**, hypothesizing that interaction with the unique R54 could achieve BRDT-1 selectivity.

2.1 Chemistry

As depicted in Scheme 1, the targeted ester analogs were generated via a multi-component reaction between *p*-tolualdehyde, 6-amino-1-ethyluracil, and various substituted 3-oxobutanoate esters. The amide analogs were synthesized in two steps by hydrolyzing methyl ester analog **2a** to generate the carboxylic acid intermediate, which was subjected to reactions with amines to yield the desired amide analogs.

2.2 Biology

We designed and synthesized nine ester (**2a-i**) and seven amide analogs (**3a-g**) with varying side chains and tested them for BRDT-1 and BRD4-1 inhibition in an AlphaScreen assay to characterize their affinity and selectivity profiles.

In the ester subset, the affinity profile (Table 1) revealed that linear aliphatic side chains (analog **2a**, **2b**, and **2c**) were tolerated, but the branched *tert*-butyl moiety (**2d**) caused a 2-fold decrease in BRDT-1 affinity, compared to lactone **1**. A more than 5-fold affinity improvement for both BRDT-1 and BRD4-1 was achieved once a benzyl moiety (analog **2e**) was introduced. Introduction of electron-donating methoxy or an electron-withdrawing chlorine on the aryl ring led to affinity loss, as exemplified for analogs **2f** and **2g**. In addition, comparison between **2g**, **2h**, and **2i** revealed that di-substitution and linker extension had marginal effects on affinity. Based on the observed BRDT-1 and BRD4-1 affinities across the series, we concluded that the introduction of an ester side chain did not provide high BRDT-1 or BRD4-1 affinity and selectivity.

To ascertain whether these analogs retained BET bromodomain selectivity, compound **2e**, the most potent ester analog was selected for BROMOscan (Eurofins) testing at 20 μ M. As shown in Figure 3, compound **2e** was highly selective for the BET bromodomain family, similar to the original hit compound **1**.

For the amide series, we noticed greater affinity losses (Table 2) compared to lactone **1** and esters **2**. The flexible and hydrophobic *n*-propyl moiety (analog **3a**) led to the most significant affinity decrease, which was rescued by introducing an allyl group (analog **3b**). Additionally, the benzyl moiety (analog **3c**), which had improved affinity in the ester series, or the surrogate phenylhydrazine moiety (analog **3d**) did not yield significant improvements. Comparison between analogs **3c**, **3e**, and **3g** indicated that extension of the amide linker was tolerated. As observed in the ester series, methoxy decoration on the aryl ring (analog **3f**), albeit tolerated, had minimal impact on the affinity. Regarding BET selectivity, we surmised that there was no significant BET selectivity among the amide analogs.

To rationalize the structure-activity relationships, we co-crystallized analog **2c** with BRD4-1 and BRDT-1. As shown in Figures 4 A and B, the allyl motif was located next to the ZA loop and was solvent exposed, thus not likely to form additional contacts with surrounding

residues. As shown in Figure 4B, the distance between the allyl group and R54 is more than 10 Å. The side chain of R54 is solvent exposed and highly flexible, and it adopts different conformations in known BRDT-1 cocrystal structures. In the cocrystal structure with **2c**, R54 extends away from the KAc site and towards solvent. The electron density of R54 is well defined and not influenced by crystal packing, suggesting an energy-low conformation of R54 in this inhibitor complex. Due to this conformation, it would be difficult for any ester analog to interact with the unique R54 in BRDT-1, explaining why no BRDT-1 specificity was achieved.

3 CONCLUSION

In summary, we conducted a structure-activity exploration using a ring-opening strategy based on previously identified lactone scaffold **1**, aiming to explore interactions with dissimilar residues at the entrance of the otherwise highly conserved Kac site of BET bromodomains. Nine ester and seven amide analogs were designed and synthesized, among which benzyl ester analog **2e** displayed the highest affinity for BRD4-1 and BRDT-1. Profiling across bromodomains demonstrated high selectivity of **2e** for the BET bromodomain family. Cocrystal structures of analog **2c** with BRD4-1 and BRDT-1 explain the lack of intra-BET selectivity of this inhibitor series.

4 EXPERIMENTAL

4.1 Chemistry

4.1.1 General—All chemicals and solvents were purchased from commercial suppliers and directly used without further purification unless otherwise specified. Reactions were monitored by TLC on 0.2 mm silica gel plates (Merck Kieselgel GF254) and visualized under UV light (254 nm). Flash column chromatography was conducted using medium-pressure liquid chromatography (MPLC) on a CombiFlash Companion (Teledyne ISCO) with pre-packed silica columns (20–40 microns) and UV detection at 254 nm. ¹H and ¹³C NMR spectra (see the Supporting Information) were performed on a Bruker 400/100 MHz Avance spectrometer. Chemical shifts are reported in ppm and referenced to residual solvent peaks (7.26 in CDCl₃, 2.50 in DMSO-*d*₆). Splitting patterns are designed as singlet (s), doublet (d), triplet (t), quartet (q), multiplet (m), and broad singlet (br). Purities of tested compounds were determined by qNMR, using DMSO₂ as the internal standard and the qNMR protocol published in the *Journal of Medicinal Chemistry*.^[44, 45]

The InChI codes of the investigated compounds, together with some biological activity data, are provided as Supporting Information.

4.1.2 General procedure A for the ring-open ester analogs—Appropriately substituted 3-oxobutanoate ester (1 equiv), *p*-tolualdehyde (1 equiv), and 6-amino-1-ethyluracil (1 equiv) were added to a dry microwave vial (5 mL). After adding AcOH (1 mL), the vial was flushed with nitrogen gas for 1 min and sealed. The mixture was heated at 110 °C for 6 h, which generated a clear yellow solution. Upon the completion monitored by TLC, the AcOH was evaporated under a nitrogen flow and the resulting solid was purified

by flash column chromatography (40 gram RediSep Gold silica gel column, DCM + 5% methanol) to give the target ring-open ester analogs.

Methyl 1-ethyl-7-methyl-2,4-dioxo-5-(*p*-tolyl)-1,2,3,4,5,8-hexahydropyrido[2,3-*d*]pyrimidine-6-carboxylate (2a): The title compound was prepared via general procedure A as a colorless solid (28 mg, 32%); mp 288–289 °C dec; with a purity 96% determined by qNMR. ¹H NMR (400 MHz, DMSO-*d*₆) δ 10.94 (s, 1H), 8.60 (s, 1H), 7.05 (d, *J* = 8.0 Hz, 2H), 7.00 (d, *J* = 8.0 Hz, 2H), 4.84 (s, 1H), 4.07–3.91 (m, 2H), 3.55 (s, 3H), 2.41 (s, 3H), 2.20 (s, 3H), 1.11 (t, *J* = 8.0 Hz, 3H). ¹³C NMR (100 MHz, DMSO-*d*₆) δ 166.9, 161.4, 149.9, 145.4, 143.9, 143.6, 135.1, 128.6, 126.9, 104.1, 90.1, 50.9, 36.2, 35.5, 20.5, 18.1, 13.7.

Propyl 1-ethyl-7-methyl-2,4-dioxo-5-*p*-tolyl-1,2,3,4,5,8-hexahydropyrido[2,3-*d*]pyrimidine-6-carboxylate (2b): The title compound was prepared via general procedure A as a colorless solid (52 mg, 54%); mp 178–180 °C dec; 96% purity determined by qNMR. ¹H NMR (400 MHz, DMSO-*d*₆) δ 10.95 (s, 1H), 8.58 (s, 1H), 7.06 (d, *J* = 8.0 Hz, 2H), 7.00 (d, *J* = 8.0 Hz, 2H), 4.84 (s, 1H), 4.02 (ddt, *J* = 27.7, 14.6, 7.2 Hz, 2H), 3.91 (t, *J* = 6.0 Hz, 2H), 2.42 (s, 3H), 2.20 (s, 3H), 1.53 (h, *J* = 7.1 Hz, 2H), 1.12 (t, *J* = 8.0 Hz, 3H), 0.80 (t, *J* = 8.0 Hz, 3H). ¹³C NMR (100 MHz, DMSO-*d*₆) δ 166.4, 161.4, 149.9, 145.3, 143.9, 143.7, 135.0, 128.5, 127.0, 104.3, 90.1, 65.0, 36.2, 35.6, 21.5, 20.6, 18.1, 13.7, 10.4.

Allyl 1-ethyl-7-methyl-2,4-dioxo-5-(*p*-tolyl)-1,2,3,4,5,8-hexahydropyrido[2,3-*d*]pyrimidine-6-carboxylate (2c): The title compound was prepared via general procedure A as a colorless solid (25.7 mg, 27%); mp 226–227 °C dec; 92% purity determined by qNMR. ¹H NMR (400 MHz, DMSO-*d*₆) δ 10.98 (s, 1H), 8.64 (s, 1H), 7.07 (d, *J* = 8.0 Hz, 2H), 7.01 (d, *J* = 8.0 Hz, 2H), 5.87 (ddt, *J* = 17.2, 10.5, 5.3 Hz, 1H, 1H), 5.19–5.12 (m, 2H), 4.87 (s, 1H), 4.50 (d, *J* = 5.3 Hz, 2H), 4.00 (dh, *J* = 28.8, 7.1 Hz, 2H), 2.43 (s, 3H), 2.20 (s, 3H), 1.11 (t, *J* = 8.0 Hz, 3H). ¹³C NMR (100 MHz, DMSO-*d*₆) δ 166.0, 161.4, 150.0, 145.8, 143.9, 143.6, 135.1, 132.9, 128.6, 127.0, 117.2, 103.9, 90.1, 63.9, 36.2, 35.5, 20.6, 18.2, 13.7.

***tert*-Butyl 1-ethyl-7-methyl-2,4-dioxo-5-*p*-tolyl-1,2,3,4,5,8-hexahydropyrido[2,3-*d*]pyrimidine-6-carboxylate (2d):** The title compound was prepared via general procedure A as a colorless solid (31 mg, 31%); mp 286–288 °C dec; 90% purity determined by qNMR. ¹H NMR (400 MHz, DMSO-*d*₆) δ 10.90 (s, 1H), 8.45 (s, 1H), 7.06 (d, *J* = 8.0 Hz, 2H), 7.01 (d, *J* = 8.0 Hz, 2H), 4.77 (s, 1H), 4.00 (dp, *J* = 28.6, 7.2 Hz, 2H), 2.37 (s, 3H), 2.21 (s, 3H), 1.33 (s, 9H), 1.12 (t, *J* = 6.0 Hz, 3H). ¹³C NMR (100 MHz, DMSO-*d*₆) δ 165.8, 161.4, 150.0, 144.0, 143.8, 134.9, 128.4, 127.1, 105.9, 90.0, 79.2, 40.1, 36.2, 36.1, 20.6, 27.8, 18.1, 13.6.

Benzyl 1-ethyl-7-methyl-2,4-dioxo-5-(*p*-tolyl)-1,2,3,4,5,8-hexahydropyrido[2,3-*d*]pyrimidine-6-carboxylate (2e): The title compound was prepared via general procedure A as a colorless solid (50 mg, 46%); mp 306–307 °C dec, 95% purity determined by qNMR. ¹H NMR (400 MHz, DMSO-*d*₆) δ 10.98 (s, 1H), 8.66 (s, 1H), 7.31–7.27 (m, 3H), 7.18 (dd, *J* = 6.9, 2.8 Hz, 2H), 7.04 (d, *J* = 8.0 Hz, 2H), 6.98 (d, *J* = 8.0 Hz, 2H), 5.05 (q, *J* = 12.8 Hz, 2H), 4.87 (s, 1H), 4.08–3.91 (m, 2H), 2.43 (s, 3H), 2.20 (s, 3H), 1.12 (t, *J* = 6.0 Hz, 3H). ¹³C

NMR (100 MHz, DMSO- d_6) δ 166.1, 161.4, 149.8, 145.9, 143.8, 143.6, 136.4, 135.1, 128.5, 128.2, 127.7, 127.6, 127.1, 103.9, 90.1, 65.0, 36.2, 35.6, 20.6, 18.2, 13.7.

4-Chlorobenzyl 1-ethyl-7-methyl-2,4-dioxo-5-*p*-tolyl-1,2,3,4,5,8-hexahydropyrido[2,3-*d*]pyrimidine-6-carboxylate (2f): The title compound was prepared via general procedure A as a colorless solid (38 mg, 33%); mp 275–276 °C dec; 98% purity determined by qNMR. ^1H NMR (400 MHz, DMSO- d_6) δ 10.96 (s, 1H), 8.64 (s, 1H), 7.36 (d, J = 7.8 Hz, 2H), 7.20 (d, J = 8.0 Hz, 2H), 7.04 (d, J = 7.8 Hz, 2H), 6.99 (d, J = 8.0 Hz, 2H), 5.04 (q, J = 12.8 Hz, 2H), 4.86 (s, 1H), 4.00 (dh, J = 28.7, 7.1 Hz, 2H), 2.44 (s, 3H), 2.22 (s, 3H), 1.12 (t, J = 8.0 Hz, 3H). ^{13}C NMR (100 MHz, DMSO- d_6) δ 166.0, 161.4, 149.8, 146.1, 143.8, 143.6, 135.6, 135.1, 132.3, 129.6, 128.5, 128.2, 127.1, 103.8, 90.2, 64.2, 36.2, 35.6, 20.6, 18.2, 13.7.

4-Methoxybenzyl 1-ethyl-7-methyl-2,4-dioxo-5-*p*-tolyl-1,2,3,4,5,8-hexahydropyrido[2,3-*d*]pyrimidine-6-carboxylate (2g): The title compound was prepared via general procedure A as a light-yellow solid (45 mg, 39%); mp 241–242 °C dec; 94% purity determined by qNMR. ^1H NMR (400 MHz, DMSO- d_6) δ 10.94 (s, 1H), 8.61 (s, 1H), 7.18 (d, J = 8.6 Hz, 2H), 7.02 (d, J = 8.1 Hz, 2H), 6.98 (d, J = 8.1 Hz, 2H), 6.89 (d, J = 8.6 Hz, 2H), 4.97 (s, 2H), 4.83 (s, 1H), 3.99 (ddt, J = 28.8, 14.2, 7.1 Hz, 2H), 3.75 (s, 3H), 2.42 (s, 3H), 2.21 (s, 3H), 1.12 (t, J = 8.0 Hz, 3H). ^{13}C NMR (100 MHz, DMSO- d_6) δ 166.2, 161.4, 159.0, 145.0, 145.6, 143.9, 143.6, 135.1, 129.7, 128.5, 128.2, 127.1, 113.7, 104.1, 90.0, 64.9, 55.0, 36.2, 35.6, 20.6, 18.1, 13.6.

3,4-Dimethoxybenzyl 1-ethyl-7-methyl-2,4-dioxo-5-*p*-tolyl-1,2,3,4,5,8-hexahydropyrido[2,3-*d*]pyrimidine-6-carboxylate (2h): The title compound was prepared via general procedure A as a colorless solid (50 mg, 41%); mp 219–220 °C dec; 97% purity determined by qNMR. ^1H NMR (400 MHz, DMSO- d_6) δ 10.95 (s, 1H), 8.62 (s, 1H), 7.02 (d, J = 8.1 Hz, 2H), 6.97 (d, J = 8.0 Hz, 2H), 6.90 (d, J = 8.2 Hz, 1H), 6.83 (s, 1H), 6.80 (d, J = 8.1 Hz, 1H), 4.97 (d, J = 4.0 Hz, 2H), 4.86 (s, 1H), 4.01 (dh, J = 28.1, 7.0 Hz, 2H), 3.74 (s, 3H), 3.69 (s, 3H), 2.43 (s, 3H), 2.21 (s, 3H), 1.12 (t, J = 6.0 Hz, 3H). ^{13}C NMR (100 MHz, DMSO- d_6) δ 166.2, 161.4, 149.9, 148.5, 145.7, 143.9, 143.6, 135.1, 128.6, 128.5, 127.0, 120.6, 111.9, 111.5, 104.0, 90.1, 65.2, 55.4, 55.3, 36.2, 35.5, 21.0, 20.5, 18.2, 13.7.

4-Methoxyphenethyl 1-ethyl-7-methyl-2,4-dioxo-5-*p*-tolyl-1,2,3,4,5,8-hexahydropyrido[2,3-*d*]pyrimidine-6-carboxylate (2i): The title compound was prepared via general procedure A as a colorless solid (61 mg, 51%); mp 140–142 °C dec; 99% purity determined by qNMR. ^1H NMR (400 MHz, DMSO- d_6) δ 10.94 (s, 1H), 8.57 (s, 1H), 7.08 (d, J = 8.5 Hz, 2H), 7.02 (d, J = 8.2 Hz, 2H), 6.99 (d, J = 8.2 Hz, 2H), 6.81 (d, J = 8.5 Hz, 2H), 4.84 (s, 1H), 4.14 (tt, J = 6.8, 3.4 Hz, 2H), 4.00 (dp, J = 28.3, 7.4 Hz, 2H), 3.96 (s, 3H), 2.78 (td, J = 6.9, 2.9 Hz, 2H), 2.36 (s, 3H), 2.21 (s, 3H), 1.11 (t, J = 6.0 Hz, 3H). ^{13}C NMR (100 MHz, DMSO- d_6) δ 166.4, 161.4, 157.7, 149.9, 145.4, 143.9, 143.6, 135.0, 129.9, 129.7, 128.5, 127.0, 126.9, 113.6, 104.2, 90.2, 64.5, 36.2, 35.5, 33.5, 20.5, 18.1, 13.6.

4.1.3 General procedure B for the synthesis of ring-open amide analogs—
Synthesis of the amide analogs starts with the hydrolysis of methyl ester analog **2a**. NaOH (4 equiv) was added to an aqueous solution of **2a**. After stirring for 18 h at rt, the resulting solution was acidified with AcOH and extracted with DCM three times. The combined

organic layer was washed with brine, dried over anhydrous MgSO₄, and concentrated under reduced pressure to yield the crude acid intermediate, which was dissolved in DMF and cooled to 0 °C. DIPEA (1 equiv), EDCI (1 equiv), HOBt (1 equiv), and the amine (1 equiv) were added successively and then the reaction mixture was stirred for 3 h at rt. Upon completion of the reaction, monitored by TLC, the mixture was poured into water and extracted with diethyl ether. The separated organic layer was washed with water and brine, dried over anhydrous MgSO₄, and concentrated under reduced pressure to obtain the crude solid product, which was purified by flash column chromatography eluting with a mixture of MeOH and DCM to give the target amide analogs.

1-Ethyl-7-methyl-2,4-dioxo-N-propyl-5-(p-tolyl)-1,2,3,4,5,8-hexahydropyrido[2,3-d]pyrimidine-6-carboxamide (3a): The title compound was prepared

via general procedure B and obtained as a colorless solid (20.1 mg, 21%); mp 121–122 °C dec; 96% purity determined by qNMR.

¹H NMR (400 MHz, DMSO-*d*₆) δ 10.78 (s, 1H), 8.11 (s, 1H), 7.65 (t, *J* = 6.0 Hz, 1H), 7.04 (d, *J* = 8.0 Hz, 2H), 7.00 (d, *J* = 8.0 Hz, 2H), 4.78 (s, 1H), 4.02–3.93 (m, 2H), 2.97 (dh, *J* = 25.9, 6.4 Hz, 2H), 2.21 (s, 3H), 2.09 (s, 3H), 1.33 (h, *J* = 7.2 Hz, 2H), 1.12 (t, *J* = 8.0 Hz, 3H), 0.74 (t, *J* = 8.0 Hz, 3H). ¹³C NMR (100 MHz, DMSO-*d*₆) δ 167.6, 161.4, 150.0, 144.9, 143.1, 134.8, 132.9, 128.4, 127.1, 111.4, 88.0, 40.4, 37.6, 36.0, 22.2, 20.5, 17.2, 13.6, 11.3.

N-Allyl-1-ethyl-7-methyl-2,4-dioxo-5-p-tolyl-1,2,3,4,5,8-hexahydropyrido[2,3-d]pyrimidine-6-carboxamide (3b): The title compound was

prepared via general procedure B and obtained as a colorless solid (30 mg, 32%); mp 115–116 °C dec; 97% purity determined by qNMR. ¹H NMR (400 MHz, DMSO-*d*₆) δ 10.80 (s, 1H), 8.15 (s, 1H), 7.85 (t, *J* = 6.0 Hz, 1H), 7.07 (d, *J* = 8.0 Hz, 2H), 7.01 (d, *J* = 8.0 Hz, 2H), 5.71 (ddt, *J* = 17.3, 10.4, 5.2 Hz, 1H), 4.95–4.86 (m, 2H), 4.82 (s, 1H), 4.00 (dh, *J* = 28.9, 7.1 Hz, 2H), 3.70–3.57 (m, 2H), 2.20 (s, 3H), 2.10 (s, 3H), 1.11 (t, *J* = 8.0 Hz, 3H). ¹³C NMR (100 MHz, DMSO-*d*₆) δ 167.6, 161.4, 150.0, 144.9, 143.0, 135.4, 134.9, 133.6, 128.5, 127.2, 114.7, 110.9, 88.2, 41.0, 37.6, 36.0, 20.6, 17.3, 13.6.

N-Benzyl-1-ethyl-7-methyl-2,4-dioxo-5-p-tolyl-1,2,3,4,5,8-hexahydropyrido[2,3-d]pyrimidine-6-carboxamide (3c): The title compound was prepared

via general procedure B and obtained as a colorless solid (40 mg, 37%); mp 239–240 °C dec; 90% purity determined by qNMR. ¹H NMR (400 MHz, DMSO-*d*₆) δ 10.79 (s, 1H), 8.21 (t, *J* = 6.0 Hz, 1H), 8.13 (s, 1H), 7.21–7.17 (m, 2H), 7.06 (d, *J* = 8.1 Hz, 2H), 7.03–6.97 (m, 4H), 4.84 (s, 1H), 4.24 (t, *J* = 6.0 Hz, 2H), 3.98 (dh, *J* = 28.6, 7.1 Hz, 2H), 2.24 (s, 3H), 2.12 (s, 3H), 1.13 (t, *J* = 6.0 Hz, 3H). ¹³C NMR (100 MHz, DMSO-*d*₆) δ 167.7, 161.4, 150.0, 144.8, 143.0, 139.6, 134.9, 133.6, 128.4, 127.9, 127.4, 126.9, 126.4, 110.9, 88.1, 42.0, 37.7, 36.0, 20.6, 17.3, 13.6.

1-Ethyl-7-methyl-2,4-dioxo-N'-phenyl-5-p-tolyl-1,2,3,4,5,8-hexahydropyrido[2,3-d]pyrimidine-6-carbohydrazide (3d): The title compound was prepared

via general procedure B and obtained as a colorless solid (17 mg, 16%), mp 164–165 °C dec, 94% purity determined by qNMR. ¹H NMR (400 MHz, DMSO-*d*₆) δ 10.80 (s, 1H), 9.49 (d, *J* = 4.0 Hz, 1H), 8.19 (s, 1H), 7.61 (d, *J* = 4.0 Hz, 1H), 7.13 (d,

$J = 8.0$ Hz, 2H), 7.06 (d, $J = 8.0$ Hz, 2H), 6.99–6.95 (m, 2H), 6.62 (t, $J = 8.0$ Hz, 1H), 6.36 (d, $J = 8.0$ Hz, 2H), 4.83 (s, 1H), 4.05–3.95 (m, 2H), 2.26 (s, 3H), 2.17 (s, 3H), 1.14 (t, $J = 6.0$ Hz, 3H). ^{13}C NMR (100 MHz, DMSO- d_6) δ 167.9, 161.3, 149.9, 149.3, 144.6, 142.9, 135.0, 133.8, 128.4, 128.3, 127.7, 118.1, 112.1, 109.4, 88.2, 37.9, 36.1, 20.6, 17.4, 13.6.

1-Ethyl-7-methyl-2,4-dioxo-N-phenethyl-5-p-tolyl-1,2,3,4,5,8-hexahydropyrido[2,3-*d*]pyrimidine-6-carboxamide (3e): The title compound was prepared

via general procedure B and obtained as a colorless solid (62 mg, 56%); mp 194–195 °C dec; 97% purity determined by qNMR. ^1H NMR (400 MHz, DMSO- d_6) δ 10.78 (s, 1H), 8.12 (s, 1H), 7.71 (t, $J = 6.0$ Hz, 1H), 7.24 (t, $J = 7.4$ Hz, 2H), 7.17 (t, $J = 7.2$ Hz, 1H), 7.10 (d, $J = 8.2$ Hz, 2H), 7.02 (d, $J = 8.1$ Hz, 2H), 6.99 (d, $J = 8.1$ Hz, 2H), 4.76 (s, 1H), 3.97 (dh, $J = 29.2, 7.1$ Hz, 2H), 3.26 (dq, $J = 13.9, 6.9$ Hz, 2H), 2.65 (hept, $J = 6.7$ Hz, 2H), 2.21 (s, 3H), 2.03 (s, 3H), 1.12 (t, $J = 6.0$ Hz, 3H). ^{13}C NMR (100 MHz, DMSO- d_6) δ 167.7, 161.4, 150.0, 144.8, 142.9, 139.4, 134.8, 133.6, 128.5, 128.4, 128.2, 127.1, 125.9, 111.0, 88.1, 40.3, 37.5, 36.0, 34.9, 20.6, 17.2, 13.6.

1-Ethyl-N-(4-methoxyphenethyl)-7-methyl-2,4-dioxo-5-p-tolyl-1,2,3,4,5,8-hexahydropyrido[2,3-*d*]pyrimidine-6-carboxamide (3f): The title

compound was prepared via general procedure B and obtained as a colorless solid (78 mg, 66%); mp 152–153 °C dec; 95% purity determined by qNMR. ^1H NMR (400 MHz, DMSO- d_6) δ 10.81 (s, 1H), 8.13 (s, 1H), 7.70 (t, $J = 6.0$ Hz, 1H), 7.04–6.99 (m, 6H), 6.80 (d, $J = 8.5$ Hz, 2H), 4.77 (s, 1H), 3.98 (ddt, $J = 35.3, 13.0, 6.6$ Hz, 2H), 3.71 (s, 3H), 3.21 (tt, $J = 13.8, 7.0$ Hz, 2H), 2.59 (h, $J = 6.6$ Hz, 2H), 2.22 (s, 3H), 2.05 (s, 3H), 1.12 (t, $J = 6.0$ Hz, 3H). ^{13}C NMR (100 MHz, DMSO- d_6) δ 167.6, 161.4, 157.5, 150.0, 144.9, 143.0, 134.8, 133.6, 131.3, 129.5, 128.5, 127.1, 113.6, 111.0, 88.1, 54.9, 40.5, 37.4, 36.0, 34.1, 20.6, 17.2, 13.6.

1-Ethyl-7-methyl-2,4-dioxo-N-(3-phenylpropyl)-5-p-tolyl-1,2,3,4,5,8-hexahydropyrido[2,3-*d*]pyrimidine-6-carboxamide (3g): The

title compound was prepared via general procedure B and obtained as a light-yellow solid (32 mg, 28%); mp 113–114 °C dec; 98% purity determined by qNMR. ^1H NMR (400 MHz, DMSO- d_6) δ 10.79 (s, 1H), 8.12 (s, 1H), 7.71 (t, $J = 4.0$ Hz, 1H), 7.25 (t, $J = 7.4$ Hz, 2H), 7.15 (t, $J = 7.3$ Hz, 1H), 7.11–7.06 (m, 4H), 6.99 (d, $J = 7.9$ Hz, 2H), 4.82 (s, 1H), 4.00 (dh, $J = 28.2, 7.1$ Hz, 2H), 3.04 (ddq, $J = 19.6, 12.8, 6.5$ Hz, 2H), 2.41 (t, $J = 7.8$ Hz, 2H), 2.19 (s, 3H), 2.11 (s, 3H), 1.61 (p, $J = 7.8$ Hz, 2H), 1.13 (t, $J = 6.0$ Hz, 3H). ^{13}C NMR (100 MHz, DMSO- d_6) δ 167.7, 161.4, 150.0, 144.9, 143.0, 141.8, 134.9, 133.1, 128.4, 128.19, 128.15, 127.2, 125.6, 111.2, 88.0, 38.2, 37.7, 36.0, 32.5, 30.9, 20.5, 17.2, 13.6.

4.2 AlphaScreen

All analogs were tested in duplicate. BRD4-1 and BRDT-1 AlphaScreen^[46] assays were performed with minimal modifications from the manufacturer's protocol (PerkinElmer, USA). All reagents were diluted in 50 mM HEPES, 150 mM NaCl, 0.1% w/v BSA, 0.01% w/v Tween 20, pH 7.5 and allowed to equilibrate to rt prior to addition to plates. After the addition of Alpha beads to the master solutions, all subsequent steps were performed under low light conditions. A 2x solution of components with final concentrations of His-BRD4 or His-BRDT at 40 nM, Ni-coated Acceptor Bead at 25 $\mu\text{g}/\text{mL}$, and 20 nM

biotinylated-JQ1(S) was added in 10 μ L to 384-well plates (AlphaPlate-384, PerkinElmer, USA). Plates were spun down at 150 \times g, after which 100 nL of compound in DMSO from stock plates were added by pin transfer using a Janus Workstation (PerkinElmer, USA). The streptavidin-coated donor beads (25 μ g/mL final) were added in the same manner as the previous solution, in a 2x solution of 10 μ L volume. Following this addition, plates were sealed with foil to prevent light exposure and evaporation. The plates were spun down again at 150 \times g. Plates were incubated at rt for 1 h and then read on an Envision 2104 (PerkinElmer, USA) plate reader using the manufacturer's protocol.

4.3 Protein crystallization and crystallography

BRD4-BD1 and BRDT-BD1 were expressed and purified as described.^[47] Crystals were grown in the presence of 1 mM **2c** by vapor-diffusion in hanging drops using precipitant 0.2 M ammonium sulfate, 0.1 M TRIS pH 8.5, 25% (w/v) polyethylene glycol 3,350 for BRD4-1, and 0.2 M lithium sulfate monohydrate, 0.1 M BIS-TRIS pH 6.5, 25% (w/v) polyethylene glycol 3,350 for BRDT-1. Crystals were harvested in cryoprotectant (precipitant + 25% (v/v) ethylene glycol) and flash frozen in a stream of nitrogen gas. X-ray diffraction data were recorded at beamline 22-BM (SER-CAT) of the Advanced Photon Source. Data were reduced and scaled with XDS.^[48] PHENIX^[49] was employed for phasing and refinement, and model building was performed using Coot.^[50] The structures were solved by molecular replacement using PDB entries 5VBP and 4KCX as search models for BRD4 and BRDT, respectively. An initial model of the inhibitor was generated with ligand restraints from eLBOW of the PHENIX suite. All structures were validated by MolProbity^[51] and phenix.model_vs_data.^[52] 2D interaction diagrams were computed with Poseview.^[43] Data collection and refinement statistics are shown in Supplementary Table S1. Atomic coordinates and structure factors have been deposited in the Protein Data Bank (PDB) under accession codes 7UTY and 7UUU.

Supplementary Material

Refer to Web version on PubMed Central for supplementary material.

ACKNOWLEDGEMENTS

This project was supported by the NIH/NICHD: HHSN275201300017C and P50HD093540 from the Contraception Research Branch.

References:

- [1]. Zeng L, Zhou M-M, FEBS Lett. 2002, 513, 124–128. [PubMed: 11911891]
- [2]. Filippakopoulos P, Picaud S, Mangos M, Keates T, Lambert JP, Barsyte-Lovejoy D, Felletar I, Volkmer R, Muller S, Pawson T, Gingras AC, Arrowsmith CH, Knapp S, Cell 2012, 149, 214–231. [PubMed: 22464331]
- [3]. Shang E, Nickerson HD, Wen D, Wang X, Wolgemuth DJ, Development 2007, 134, 3507–3515. [PubMed: 17728347]
- [4]. Zhang Q, Zeng L, Shen C, Ju Y, Konuma T, Zhao C, Vakoc CR, Zhou MM, Structure 2016, 24, 1201–1208. [PubMed: 27291650]

- [5]. Wai DCC, Szyszka TN, Campbell AE, Kwong C, Wilkinson-White LE, Silva APG, Low JKK, Kwan AH, Gamsjaeger R, Chalmers JD, Patrick WM, Lu B, Vakoc CR, Blobel GA, Mackay JP, *J. Biol. Chem* 2018, 293, 7160–7175. [PubMed: 29567837]
- [6]. Lambert JP, Picaud S, Fujisawa T, Hou H, Savitsky P, Uuskula-Reimand L, Gupta GD, Abdouni H, Lin ZY, Tucholska M, Knight JDR, Gonzalez-Badillo B, St-Denis N, Newman JA, Stucki M, Pelletier L, Bandeira N, Wilson MD, Filippakopoulos P, Gingras AC, *Mol. Cell* 2019, 73, 621–638 e617. [PubMed: 30554943]
- [7]. Jang MK, Mochizuki K, Zhou M, Jeong HS, Brady JN, Ozato K, *Mol. Cell* 2005, 19, 523–534. [PubMed: 16109376]
- [8]. Liu W, Ma Q, Wong K, Li W, Ohgi K, Zhang J, Aggarwal A, Rosenfeld MG, *Cell* 2013, 155, 1581–1595. [PubMed: 24360279]
- [9]. Rahman S, Sowa ME, Ottinger M, Smith JA, Shi Y, Harper JW, Howley PM, *Mol Cell Biol* 2011, 31, 2641–2652. [PubMed: 21555454]
- [10]. Fukazawa H, Masumi A, *Biol. Pharm. Bull* 2012, 35, 2064–2068. [PubMed: 22971749]
- [11]. Delmore JE, Issa GC, Lemieux ME, Rahl PB, Shi J, Jacobs HM, Kastriitis E, Gilpatrick T, Paranal RM, Qi J, Chesi M, Schinzel AC, McKeown MR, Heffernan TP, Vakoc CR, Bergsagel PL, Ghobrial IM, Richardson PG, Young RA, Hahn WC, Anderson KC, Kung AL, Bradner JE, Mitsiades CS, *Cell* 2011, 146, 904–917. [PubMed: 21889194]
- [12]. Salvatori B, Iosue I, Djodji Damas N, Mangiavacchi A, Chiaretti S, Messina M, Padula F, Guarini A, Bozzoni I, Fazi F, Fatica A, *Genes Cancer* 2011, 2, 585–592. [PubMed: 21901171]
- [13]. Nie Z, Hu G, Wei G, Cui K, Yamane A, Resch W, Wang R, Green DR, Tessarollo L, Casellas R, Zhao K, Levens D, *Cell* 2012, 151, 68–79. [PubMed: 23021216]
- [14]. Szabo AG, Gang AO, Pedersen MO, Poulsen TS, Klausen TW, Norgaard P, *Leuk. Lymphoma* 2016, 57, 2526–2534. [PubMed: 27243588]
- [15]. Matzuk MM, McKeown MR, Filippakopoulos P, Li Q, Ma L, Agno JE, Lemieux ME, Picaud S, Yu RN, Qi J, Knapp S, Bradner JE, *Cell* 2012, 150, 673–684. [PubMed: 22901802]
- [16]. Barda S, Paz G, Yogev L, Yavetz H, Lehavi O, Hauser R, Botchan A, Breitbart H, Kleiman SE, *Fertil. Steril* 2012, 97, 46–52 e45. [PubMed: 22035730]
- [17]. Berkovits BD, Wolgemuth DJ, *Dev. Biol* 2011, 360, 358–368. [PubMed: 22020252]
- [18]. Yu Z, Ku Angela F, Anglin Justin L, Sharma R, Ucisik Melek N, Faver John C, Li F, Nyshadham P, Simmons N, Sharma Kiran L, Nagarajan S, Riehle K, Kaur G, Sankaran B, Stori-Desmond M, Palmer Stephen S, Young Damian W, Kim C, Matzuk Martin M, *PNAS* 2021, 118, e2021102118. [PubMed: 33637650]
- [19]. Filippakopoulos P, Qi J, Picaud S, Shen Y, Smith WB, Fedorov O, Morse EM, Keates T, Hickman TT, Felletar I, Philpott M, Munro S, McKeown MR, Wang Y, Christie AL, West N, Cameron MJ, Schwartz B, Heightman TD, La Thangue N, French CA, Wiest O, Kung AL, Knapp S, Bradner JE, *Nature* 2010, 468, 1067–1073. [PubMed: 20871596]
- [20]. Mirguet O, Gosmini R, Toum J, Clement CA, Barnathan M, Brusq JM, Mordaunt JE, Grimes RM, Crowe M, Pineau O, Ajakane M, Daugan A, Jeffrey P, Cutler L, Haynes AC, Smithers NN, Chung CW, Bamborough P, Uings IJ, Lewis A, Witherington J, Parr N, Prinjha RK, Nicodeme E, *J. Med. Chem* 2013, 56, 7501–7515. [PubMed: 24015967]
- [21]. McDaniel KF, Wang L, Soltwedel T, Fidanze SD, Hasvold LA, Liu D, Mantei RA, Pratt JK, Sheppard GS, Bui MH, Faivre EJ, Huang X, Li L, Lin X, Wang R, Warder SE, Wilcox D, Albert DH, Magoc TJ, Rajaraman G, Park CH, Hutchins CW, Shen JJ, Edalji RP, Sun CC, Martin R, Gao W, Wong S, Fang G, Elmore SW, Shen Y, Kati WM, *J. Med. Chem* 2017, 60, 8369–8384. [PubMed: 28949521]
- [22]. Andrieu G, Belkina AC, Denis GV, *Drug Discov. Today Technol* 2016, 19, 45–50. [PubMed: 27769357]
- [23]. Cui H, Carlson AS, Schleiff MA, Divakaran A, Johnson JA, Buchholz CR, Zahid H, Vail NR, Shi K, Aihara H, Harki DA, Miller GP, Topczewski JJ, Pomerantz WCK, *J. Med. Chem* 2021, 64, 10497–10511. [PubMed: 34236185]
- [24]. Rianjongdee F, Atkinson SJ, Chung CW, Grandi P, Gray JRJ, Kaushansky LJ, Medeiros P, Messenger C, Phillipou A, Preston A, Prinjha RK, Rioja I, Satz AL, Taylor S, Wall ID, Watson RJ, Yao G, Demont EH, *J. Med. Chem* 2021, 64, 10806–10833. [PubMed: 34251219]

- [25]. Seal JT, Atkinson SJ, Bamborough P, Bassil A, Chung CW, Foley J, Gordon L, Grandi P, Gray JRJ, Harrison LA, Kruger RG, Matteo JJ, McCabe MT, Messenger C, Mitchell D, Phillipou A, Preston A, Prinjha RK, Rianjongdee F, Rioja I, Taylor S, Wall ID, Watson RJ, Woolven JM, Wyce A, Zhang XP, Demont EH, *J. Med. Chem* 2021, 64, 10772–10805. [PubMed: 34255512]
- [26]. Lucas SCC, Atkinson SJ, Chung CW, Davis R, Gordon L, Grandi P, Gray JJR, Grimes T, Phillipou A, Preston AG, Prinjha RK, Rioja I, Taylor S, Tomkinson NCO, Wall I, Watson RJ, Woolven J, Demont EH, *J. Med. Chem* 2021, 64, 10711–10741. [PubMed: 34260229]
- [27]. Liu Z, Li Y, Chen H, Lai HT, Wang P, Wu SY, Wold EA, Leonard PG, Joseph S, Hu H, Chiang CM, Brasier AR, Tian B, Zhou J, *J. Med. Chem* 2022, 65, 2388–2408. [PubMed: 34982556]
- [28]. Gilan O, Rioja I, Knezevic K, Bell MJ, Yeung MM, Harker NR, Lam EYN, Chung CW, Bamborough P, Petretich M, Urh M, Atkinson SJ, Bassil AK, Roberts EJ, Vassiliadis D, Burr ML, Preston AGS, Wellaway C, Werner T, Gray JR, Michon AM, Gobbetti T, Kumar V, Soden PE, Haynes A, Vappiani J, Tough DF, Taylor S, Dawson SJ, Bantscheff M, Lindon M, Drewes G, Demont EH, Daniels DL, Grandi P, Prinjha RK, Dawson MA, *Science* 2020, 368, 387–394. [PubMed: 32193360]
- [29]. Faivre EJ, McDaniel KF, Albert DH, Mantena SR, Plotnik JP, Wilcox D, Zhang L, Bui MH, Sheppard GS, Wang L, Sehgal V, Lin X, Huang X, Lu X, Uziel T, Hessler P, Lam LT, Bellin RJ, Mehta G, Fidanze S, Pratt JK, Liu D, Hasvold LA, Sun C, Panchal SC, Nicolette JJ, Fossey SL, Park CH, Longenecker K, Bigelow L, Torrent M, Rosenberg SH, Kati WM, Shen Y, *Nature* 2020, 578, 306–310. [PubMed: 31969702]
- [30]. Tanaka M, Roberts JM, Seo HS, Souza A, Paulk J, Scott TG, DeAngelo SL, Dhe-Paganon S, Bradner JE, *Nat. Chem. Biol* 2016, 12, 1089–1096. [PubMed: 27775715]
- [31]. Ren C, Zhang G, Han F, Fu S, Cao Y, Zhang F, Zhang Q, Meslamani J, Xu Y, Ji D, Cao L, Zhou Q, Cheung KL, Sharma R, Babault N, Yi Z, Zhang W, Walsh MJ, Zeng L, Zhou MM, *Proc. Natl. Acad. Sci. U. S. A* 2018, 115, 7949–7954. [PubMed: 30012592]
- [32]. Sakamoto KM, Kim KB, Kumagai A, Mercurio F, Crews CM, Deshaies RJ, *Proc. Natl. Acad. Sci. U. S. A* 2001, 98, 8554–8559. [PubMed: 11438690]
- [33]. Nowak RP, DeAngelo SL, Buckley D, He Z, Donovan KA, An J, Safaee N, Jedrychowski MP, Ponthier CM, Ishoey M, Zhang T, Mancias JD, Gray NS, Bradner JE, Fischer ES, *Nat. Chem. Biol* 2018, 14, 706–714. [PubMed: 29892083]
- [34]. Postel-Vinay S, Herbschleb K, Massard C, Woodcock V, Soria JC, Walter AO, Ewerton F, Poelman M, Benson N, Ocker M, Wilkinson G, Middleton M, *Eur. J. Cancer* 2019, 109, 103–110. [PubMed: 30711772]
- [35]. Lewin J, Soria JC, Stathis A, Delord JP, Peters S, Awada A, Aftimos PG, Bekradda M, Rezai K, Zeng Z, Hussain A, Perez S, Siu LL, Massard C, *J. Clin. Oncol* 2018, 36, 3007–3014. [PubMed: 29733771]
- [36]. Piha-Paul SA, Hann CL, French CA, Cousin S, Brana I, Cassier PA, Moreno V, de Bono JS, Harward SD, Ferron-Brady G, Barbash O, Wyce A, Wu Y, Horner T, Annan M, Parr NJ, Prinjha RK, Carpenter CL, Hilton J, Hong DS, Haas NB, Markowski MC, Dhar A, O'Dwyer PJ, Shapiro GI, *JNCI Cancer Spectr.* 2020, 4, pkz093. [PubMed: 32328561]
- [37]. Ameratunga M, Brana I, Bono P, Postel-Vinay S, Plummer R, Aspegren J, Korjamo T, Snapir A, de Bono JS, *Br. J. Cancer* 2020, 123, 1730–1736. [PubMed: 32989226]
- [38]. Rathert P, Roth M, Neumann T, Muerdter F, Roe JS, Muhar M, Deswal S, Cerny-Reiterer S, Peter B, Jude J, Hoffmann T, Boryn LM, Axelsson E, Schweifer N, Tontsch-Grunt U, Dow LE, Gianni D, Pearson M, Valent P, Stark A, Kraut N, Vakoc CR, Zuber J, *Nature* 2015, 525, 543–547. [PubMed: 26367798]
- [39]. Shu S, Lin CY, He HH, Witwicki RM, Tabassum DP, Roberts JM, Janiszewska M, Huh SJ, Liang Y, Ryan J, Doherty E, Mohammed H, Guo H, Stover DG, Ekram MB, Brown J, D'Santos C, Krop IE, Dillon D, McKeown M, Ott C, Qi J, Ni M, Rao PK, Duarte M, Wu SY, Chiang CM, Anders L, Young RA, Winer E, Letai A, Barry WT, Carroll JS, Long H, Brown M, Liu XS, Meyer CA, Bradner JE, Polyak K, *Nature* 2016, 529, 413–417. [PubMed: 26735014]
- [40]. Jang JE, Eom JI, Jeung HK, Cheong JW, Lee JY, Kim JS, Min YH, *Clin. Cancer Res* 2017, 23, 2781–2794. [PubMed: 27864418]

- [41]. Ayoub AM, Hawk LML, Herzig RJ, Jiang J, Wisniewski AJ, Gee CT, Zhao P, Zhu JY, Berndt N, Offei-Addo NK, Scott TG, Qi J, Bradner JE, Ward TR, Schonbrunn E, Georg GI, Pomerantz WCK, *J. Med. Chem* 2017, 60, 4805–4817. [PubMed: 28535045]
- [42]. Miao Z, Guan X, Jiang J, Georg GI, in *Targeting Protein-Protein Interactions by Small Molecules* (Eds.: Sheng C, Georg GI), Springer Singapore, 2018, pp. 287–315.
- [43]. Stierand K, Maass PC, Rarey M, *Bioinformatics* 2006, 22, 1710–1716. [PubMed: 16632493]
- [44]. Pauli GF, Chen SN, Simmler C, Lankin DC, Godecke T, Jaki BU, Friesen JB, McAlpine JB, Napolitano JG, *J. Med. Chem* 2014, 57, 9220–9231. [PubMed: 25295852]
- [45]. Pauli GF, Chen SN, Simmler C, Lankin DC, Godecke T, Jaki BU, Friesen JB, McAlpine JB, Napolitano JG, *J. Med. Chem* 2015, 58, 9061. [PubMed: 26602703]
- [46]. Roberts JM, Bradner JE, *Curr. Protoc. Chem. Biol* 2015, 7, 263–278. [PubMed: 26629616]
- [47]. Karim RM, Bikowitz MJ, Chan A, Zhu J-Y, Grassie D, Becker A, Berndt N, Gunawan S, Lawrence NJ, Schönbrunn E, *J. Med. Chem* 2021, 64, 15772–15786. [PubMed: 34710325]
- [48]. Kabsch W, *Acta Crystallogr. D Biol. Crystallogr* 2010, 66, 125–132. [PubMed: 20124692]
- [49]. Adams PD, Afonine PV, Bunkoczi G, Chen VB, Davis IW, Echols N, Headd JJ, Hung LW, Kapral GJ, Grosse-Kunstleve RW, McCoy AJ, Moriarty NW, Oeffner R, Read RJ, Richardson DC, Richardson JS, Terwilliger TC, Zwart PH, *Acta Crystallogr. D Biol. Crystallogr* 2010, 66, 213–221. [PubMed: 20124702]
- [50]. Emsley P, Lohkamp B, Scott WG, Cowtan K, *Acta Crystallogr. D Biol. Crystallogr* 2010, 66, 486–501. [PubMed: 20383002]
- [51]. Chen VB, Arendall WB 3rd, Headd JJ, Keedy DA, Immormino RM, Kapral GJ, Murray LW, Richardson JS, Richardson DC, *Acta Crystallogr. D Biol. Crystallogr* 2010, 66, 12–21. [PubMed: 20057044]
- [52]. Afonine PV, Grosse-Kunstleve RW, Chen VB, Headd JJ, Moriarty NW, Richardson JS, Richardson DC, Urzhumtsev A, Zwart PH, Adams PD, *J. Appl. Crystallogr* 2010, 43, 669–676. [PubMed: 20648263]

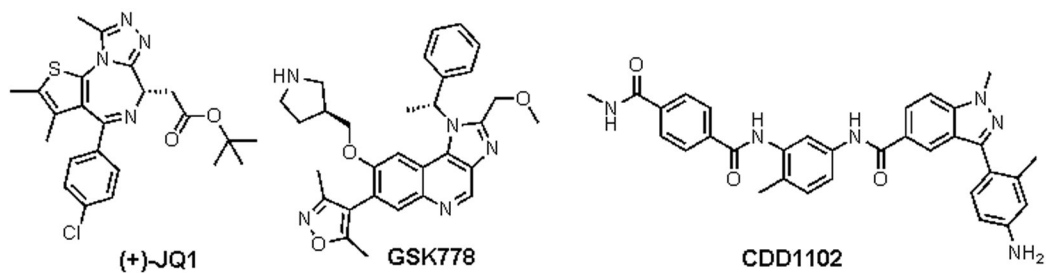
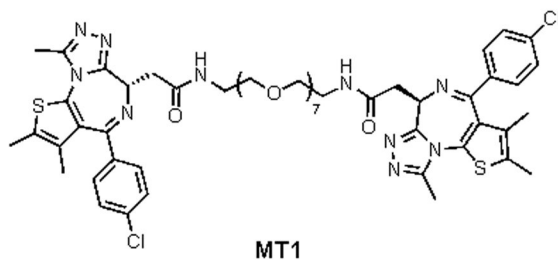
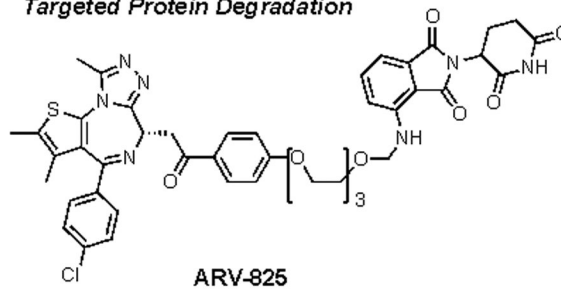
Monovalent inhibitors**Bivalent inhibitors****Targeted Protein Degradation**

Figure 1.
Reported BET inhibition strategies and representative molecules.

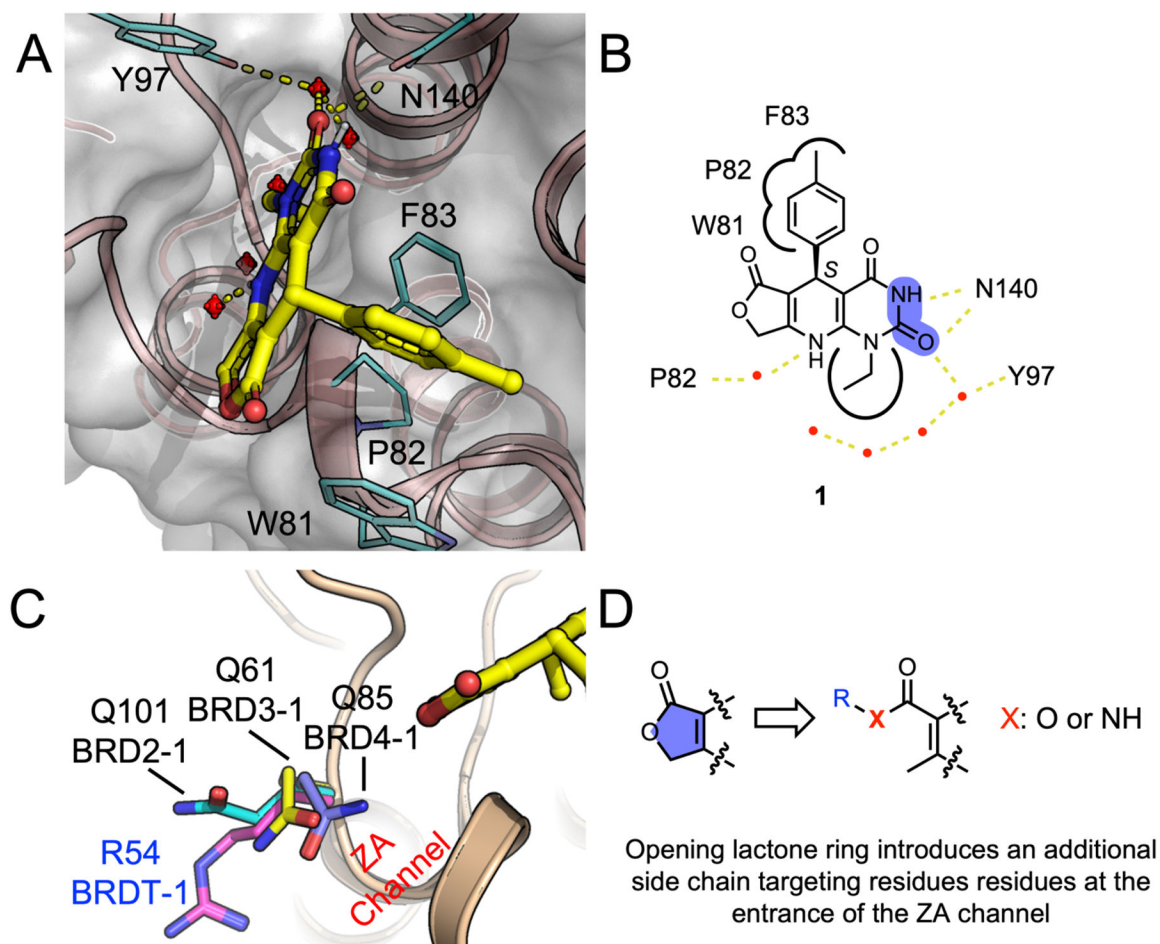


Figure 2.

The binding mode and design rationale for analogs of compound **1**. (A) The co-crystal complex of compound **1** with BRD4-1 (PDB ID: 5KDH). Key residues are denoted in cyan sticks with black text, key hydrogen bonds are highlighted in yellow dashes, and conserved water molecules are displayed in red spheres. (B) The 2D binding plot of compound **1**. (C) Superimposition of the four BD1 bromodomains of the BET family. One major difference around the recognition site lies in the ZA channel, in which BRDT-1 (PDB ID: 4FLP) has a positively charged arginine (magenta), whereas BRD2-1, BRD3-1, and BRD4-1 (PDB ID: 6DDI, 6QJU, and 5KDH) have neutral glutamines (highlighted in cyan, yellow, and purple, respectively). (D) The proposed ring-open strategy is expected to provide an additional side chain to interact with the residues at the entrance of the ZA channel.

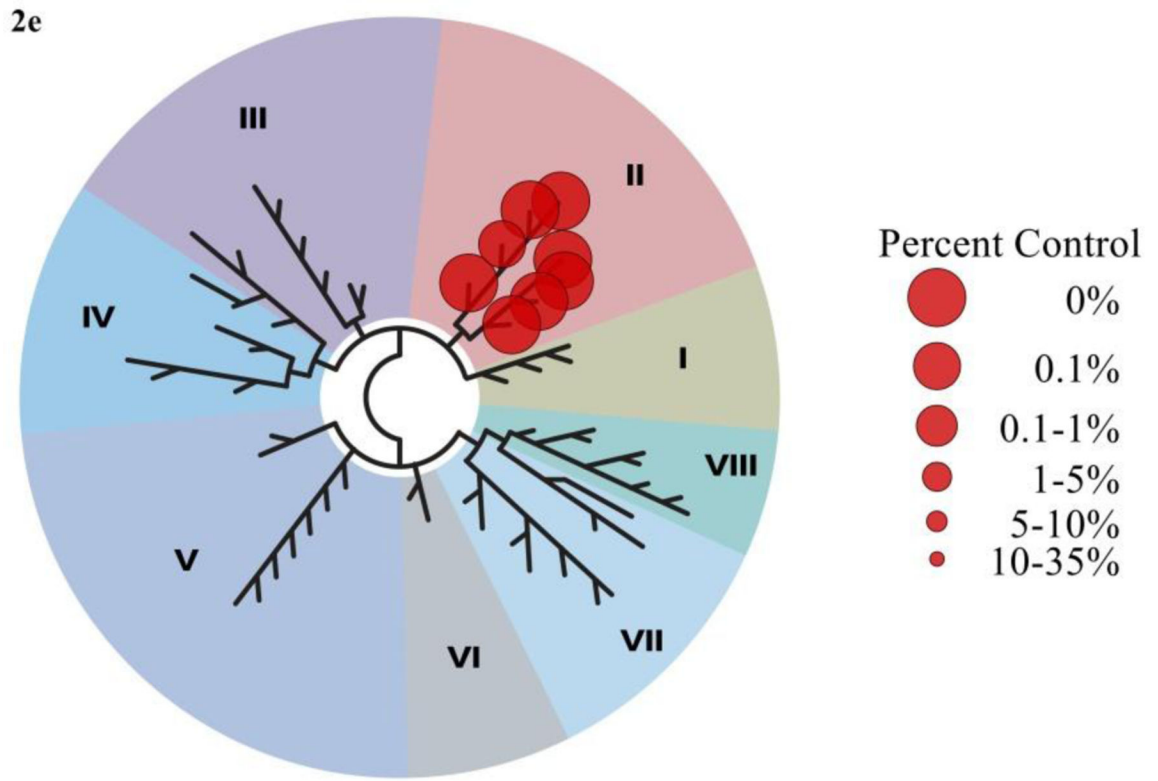


Figure 3.
BROMOscan for compound **2e**.

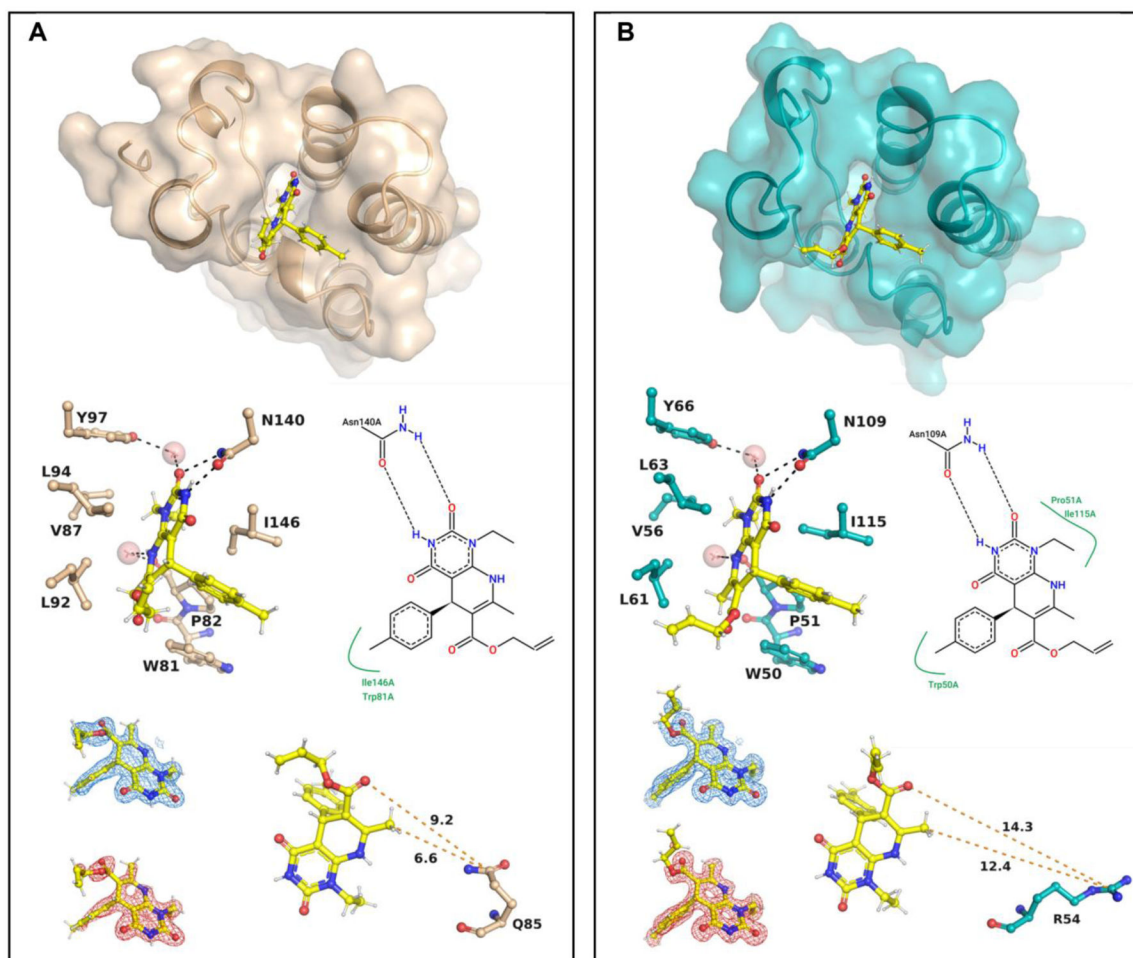
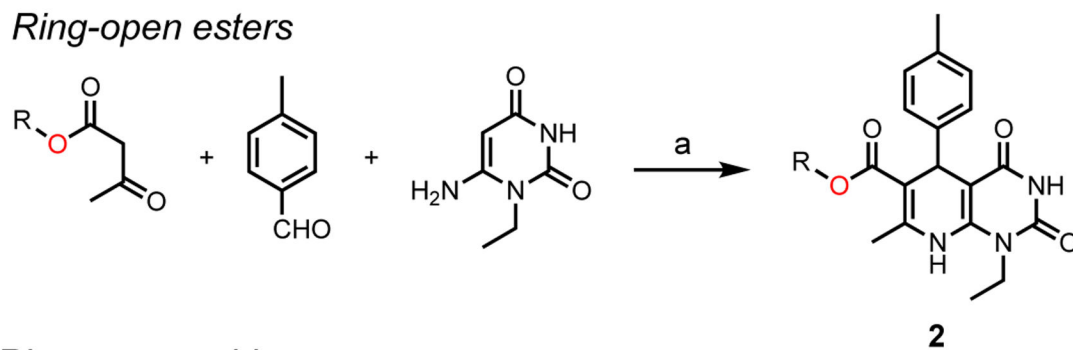
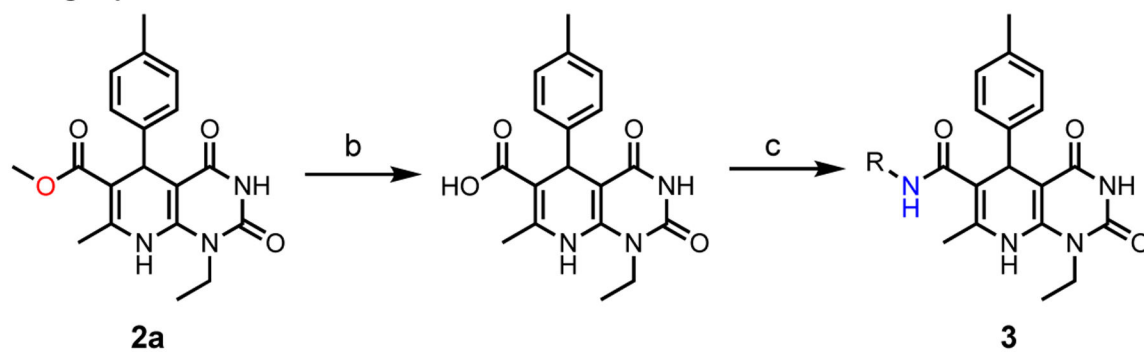


Figure 4.

Binding analysis of ring-open scaffold **2c**. (A). Cocystal structure of BRD4-1 with compound **2c** (1.55 Å). Key and surrounding residues are shown in pink. (B) Cocystal structure of BRDT-1 with compound **2c** (1.52 Å). Key and surrounding residues are shown in cyan. Hydrogen bonds are shown as black dashed lines and conserved water molecules are displayed in red spheres. 2D interaction diagrams were computed by Poseview.^[43] The blue and red mesh show the electron density upon refinement with (2Fo-Fc at 1σ) and without (Fo-Fc at 3σ) inhibitor, respectively. Distances between the ester moiety and the ZA-channel entrance residues of BRD4 (Gln85) and BRDT (Arg54) are indicated in Å.

Ring-open esters*Ring-open amides***Scheme 1.**

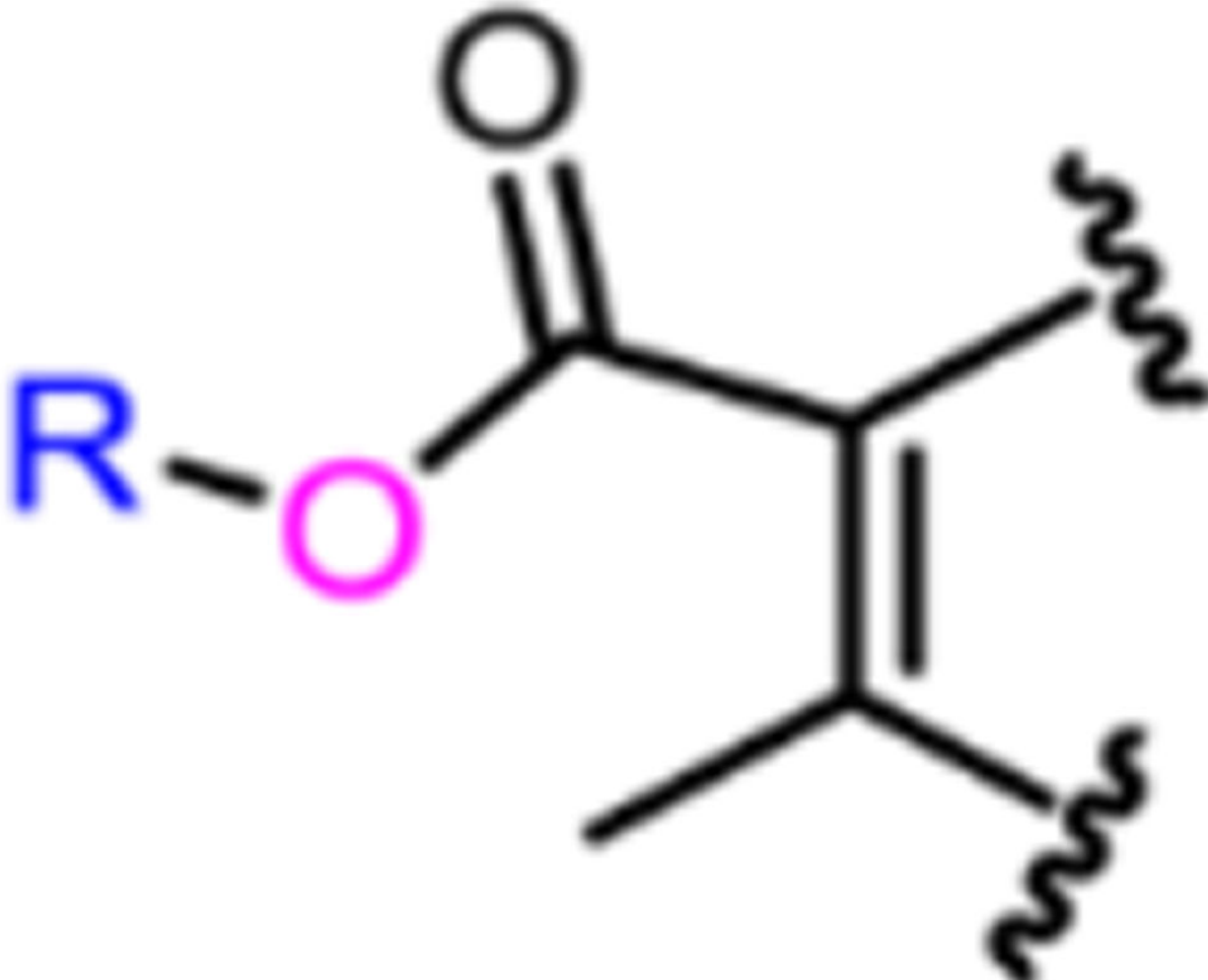
Synthesis of ester and amide analogs. Reagents and conditions: a) AcOH, reflux, 27–46%;

b) NaOH (4.0 equiv), 25 °C; c) RNH_2 (1.0 equiv), EDCI (1.0 equiv), HOBt (1.0 equiv),

DIPEA (1.0 equiv), DCM, 25 °C, 32–66% over 2 steps.

Table 1.

Structures and affinity profiles for the ester analogs

Compound	
2a	
2b	
2c	
2d	
2e	
2f	
2g	

Compound

2h

2i

1**(+)-JQ1** *

*
(+)-JQ1 was used as the positive control. All compounds were tested once in duplicate.

Author Manuscript



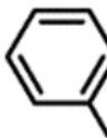
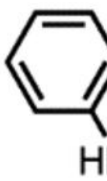
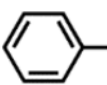
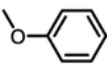
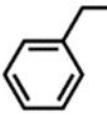
Author Manuscript

Author Manuscript

Author Manuscript

Table 2.

Structures and affinity profiles for the amide analogs

Compound	R
3a	
3b	
3c	
3d	
3e	
3f	
3g	
1	R
JQ1	

* (+)-JQ1 was used as the positive control. All compounds were tested once in duplicate.